



## A four spiral slots microstrip patch antenna for radiotelemetry capsules based on FDTD\*

HUANG Biao<sup>†</sup>, YAN Guo-zheng, LI Qian-ru

(Department of Instrument, Shanghai Jiao Tong University, Shanghai 200240, China)

<sup>†</sup>E-mail: huangb@sjtu.edu.cn

Received Dec. 27, 2006; revision accepted Apr. 18, 2007

**Abstract:** Antenna is very crucial to radiotelemetry capsules which can measure the physiological parameters of the gastrointestinal (GI) tract. The objective of this paper is to design a novel spiral slots microstrip patch antenna for the radiotelemetry capsules communicating with external recorder at 915 MHz located in ISM (Industry, Science, and Medical) bands. The microstrip patch antenna is designed and evaluated using the finite-difference time-domain (FDTD) method. Return loss characteristics and the effect of the human body on resonant frequency are analyzed, and the performances of radiation patterns at different positions of the human alimentary tract are also estimated. Finally, specific absorption rate (SAR) computations are performed, and the peak 1-g and 10-g SAR values are calculated. According to the peak SAR values, the maximum delivered power for the designed antenna was found so that the SAR values of the antenna satisfy the ANSI (American National Standards Institute) limitations.

**Key words:** Finite-difference time-domain (FDTD), Microstrip patch antenna, Specific absorption rate (SAR), Radiotelemetry capsule

doi:10.1631/jzus.2007.A1560

Document code: A

CLC number: TN82

### INTRODUCTION

There is great potential in developing non-invasive microelectronic capsules capable of monitoring physiological parameters of the gastrointestinal (GI) tract. In recent years, the interest in endoscopic radiosondes increased significantly, with efforts from various research centers and commercial institutions. Now, different physiological parameters, including temperature, chemical concentrations and images, can be captured within the GI tract (Iddan *et al.*, 2000; Pandolfino *et al.*, 2003; Wang *et al.*, 2005; Johannessen *et al.*, 2006), and the data relayed wirelessly to a body-worn device (external recorder). Since the radiotelemetry capsule's first appearance, many research groups have been working on the system, hoping to further improve the performances of the system, including reducing sizes, speeding up trans-

mission rate, improving sampling precision and so on. However, there were few investigations on radio capsule's antenna and specific absorption rate (SAR) distributions of the realistic human models.

The internal RF transmitter transmits the data outside for receiving and saving through an ingested antenna. Since the capsule and its antenna are operated inside the human body, to encase the antenna size in capsule module, a very small sized antenna is required. Nevertheless, human body is composed of various body tissues in a very complicated manner. It is very difficult to determine the absorption of electromagnetic (EM) power radiated from an ingested or implanted source within the human body. So designing antenna for ingested capsule module is extremely challenging because of reduced antenna efficiency, impact of the human tissues on the antenna, the need to reduce antenna size, and the very strong effect of multipath losses. Until now, much research has been done to determine the electrical properties of individual body tissue, such as blood, muscle, fat and skin

\* Project (No. 2006AA04Z368) supported by the Hi-Tech Research and Development Program (863) of China

(Lin, 1975; Gandhi *et al.*, 1996). And some implanted antennas were developed for medical therapy and diagnosis, pacemakers, defibrillators, etc. (Kim and Rahmat-Samii, 2004; Soontornpipit *et al.*, 2004; Kim *et al.*, 2005). In accordance with the rapid development of the computer, anatomically based models of humans and animals can be incorporated into full-wave EM simulators. So far, several researchers have investigated the radiation performances of the implanted antenna and SAR distributions in human body. Scanlon and Evans (2000) analyzed the radio wave propagation characteristics of a source implanted in the vagina; Chirwa *et al.* (2003) studied the implanted source in realistic human models (a finite-difference time-domain (FDTD) mesh of a human subject) and found that the radiation field attenuates rapidly at frequency above 1 GHz, which means the radiation transmission becomes less ineffective, and may not be suitable to use.

In this paper an appropriate compact microstrip patch antenna was designed for radiotelemetry capsule communicating with external recorder devices. And the compact microstrip patch antenna operates at 915 MHz located in ISM (Industry, Science and Medical) bands. Then the radiation characteristics of the proposed antenna operating at four different positions of the alimentary canal were studied.

In recent years, there has been increasing public concern about the health implication of EM wave exposure, and safety guidelines for limiting the exposure have been issued (IEEE Standard C95.1-1999, 1999). For the evaluation of performances and safety issues related to the ingested microstrip antenna, the radiation characteristics and 1-g and 10-g averaged SAR distributions are simulated and compared with American National Standards Institute (ANSI)/IEEE limitations for SAR (IEEE Standard C95.1-1999, 1999). Finally, the maximum transmit power is obtained to guide the designs of the RF communication module.

## ANTENNA DESIGN

Microstrip antennas are popular and are getting increasing attention due to their excellent advantages. Owing to the nature of the electro-capsule, the transmitting antenna must be very compact, robust,

low profile and lightweight. Thus, microstrip patch antenna (Gupta, 1988) was selected. Methods to reduce the size of the microstrip antenna such as adding short strip, using high dielectric substrate materials, and spiral conductor shape are usually applied. In this paper, these size-reduction techniques were employed to design the compact antenna. For this study, the antenna is designed with a high dielectric constant of  $\epsilon_r=6.1$  (Macor) and a thickness of  $h=0.6$  mm.

The proposed antenna in this work is shown in Fig.1. The new antenna comprises four spiral slots in the first layer, a ground plane in the second layer, a short-circuited strip, a feed pin, and a dielectric layer. The patch in the first layer is connected to the ground plane via a vertical short-circuited strip and is fed via a feed strip connected to a 50  $\Omega$  transmission line etched on the back of the ground plane.

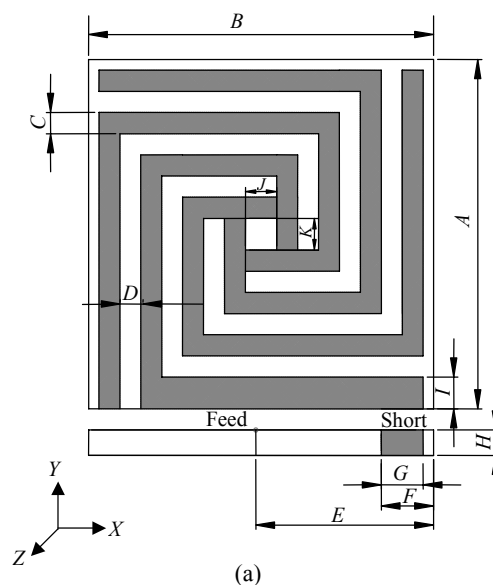


**Fig.1 The proposed spiral antenna at 915 MHz**  
(a) Design drawing; (b) Fabricated antenna

For the designed antenna, to facilitate its embedding in radiotelemetry capsules, it is essential to restrict its size approximately to within  $8.25 \times 8.25 \times 0.60 \text{ mm}^3$ . The implemented antenna is shown in Fig. 1b, and the design parameters are listed in Table 1. Due to tolerances involved during actual fabrication, the realized antenna resonated at 915~920 MHz operating in the human body. To maintain consistency of notation, the antenna will be referred to as belonging to the corresponding 915 MHz.

**Table 1 Parameters defined in Fig.1 for the proposed antenna designed at 915 MHz**

Parameter	Value (mm)	Parameter	Value (mm)
<i>A</i>	8.25	<i>G</i>	1.00
<i>B</i>	8.25	<i>H</i>	0.60
<i>C</i>	0.50	<i>I</i>	0.75
<i>D</i>	0.50	<i>J</i>	0.75
<i>E</i>	3.25	<i>K</i>	0.75
<i>F</i>	1.25		

## HUMAN MODEL AND FDTD MODELING

### Computational method

The proposed antenna does not have a regular geometric shape, hence, analytical techniques such as transmission-line model and cavity model cannot be used directly. In this paper, the FDTD method is used for investigating the interaction between the human model and the proposed antenna (Yee, 1966). The FDTD formulations were derived from Maxwell's time-domain equations by discretizing the space into a number of voxels and assigning each voxel to the corresponding permittivity and conductivity. This means that the calculation of the EM field values progresses at discrete steps in time. One benefit of the time domain approach is that it gives broadband output from a single execution of the program. Furthermore, this method adapts very well to the human models and offers great flexibility in modeling the heterogeneous structures of anatomical tissues and organs.

### Human body model

To study the interaction of the radiated EM field with an exposed subject, a heterogeneous model of a man has been used. The male human body model was

created using digitized data in the form of transverse color images from the Visible Human Project sponsored by the USA National Library of Medicine. It was generated using axial anatomical images since these had the finest resolution for the entire body in the Visible Human Project. In the project, the axial anatomical cross sections are at 1 mm intervals. And the human model is 1.80 m high and weighs 106 kg. The generated model is made up of cubic voxels with an edge size of 5 mm. Each voxel edge in the mesh is defined as one of 25 groups of tissue types. In order to incorporate the inhomogeneous human model into the FDTD scheme, the dielectric properties of the tissues are required. They are determined using the 4-Cole-Cole extrapolation (Gabriel *et al.*, 1996). Dielectric properties of human body tissues can be accessed at <http://www.brooks.af.mil/AFRL/HED/hedr/reports/dielectric/home.html>

### Computational parameters and conditions

The antenna described in this paper is excited with a gap voltage source specified with a  $50 \Omega$  series source impedance to simulate a real-voltage generator and reduce the number of time steps needed for convergence. The Gaussian pulse provides a broadband input and is suitable when results versus frequency are desired. Transient excitation using a Gaussian derivative pulse is used to calculate the wide-band input impedance. A sinusoidal input may also be chosen for cases where steady-state results are desired. Antenna far-field patterns and SAR results were calculated using a steady-state sinusoidal excitation of 915 MHz and are run for 100 000 time steps to obtain the convergence or steady-state condition. For geometries in which wave-object interaction proceeds in the open region, the computational space has to be truncated by absorbing boundaries. In this paper, the material-independent eight-layered perfectly matched layer (PML) is used as an absorbing boundary condition so that the human model can be immersed in the PML layers, as mentioned in (Berenger, 1996; Lazzi *et al.*, 2000).

As the dimensions of the antenna are much smaller than the human body model, the  $5 \times 5 \times 5 \text{ mm}^3$  cell is larger for the microstrip patch antenna. So the uniform cell grid of 5-mm resolution is not appreciated. Adaptive mesh technology can be used to solve the problem. That is, setting fine cells where the

geometry or field behavior requires high spatial resolution and larger cells elsewhere in the FDTD model. In this paper, the planes of microstrip patch antenna are made of cells with size of  $0.25 \times 0.25 \times 0.30 \text{ mm}^3$ , others made of cells with size of  $5 \times 5 \times 5 \text{ mm}^3$ .

In this paper, we only present the representative simulation results that were carried out for the ingested antenna (vertical orientation) at four locations in the GI tract (Chirwa *et al.*, 2003). These locations were: a left location, top of the small intestine (Position A); a central location, lower extent of the small intestine (Position B); right extremity of the small intestine next to the colon (Position C); lower extent of the esophageal, next to stomach (Position D). The selected four locations cover the whole extent of the alimentary canal and are representative of the overall GI tract. The surrounding tissue at each location differed significantly from those of the others, which could reflect the radiation performances of the proposed antenna. Figs.2a and 2b show the four source positions considered in vertical transverse and axial transverse cross sections, respectively.

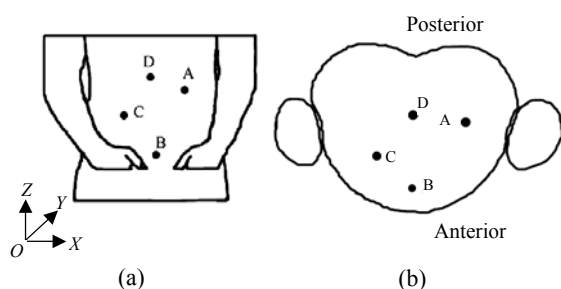


Fig.2 Locations of the ingested antenna. (a) Location in the vertical-transverse plane (subject facing toward the reader); (b) Location in the axial-transverse plane

Since the capsule casings and circuitry have been found to have negligible effect on the resident antenna's radiation, there is no need to take the effects of the casing into account in the modeling of the antenna (Chirwa *et al.*, 2003).

## RESULTS AND DISCUSSION

### Return loss characteristics

The four spiral slots design can be thought of as a modified spiral antenna, twisted up to reduce the size. The short strip acts somewhat as a ground plane on a patched inverse F antenna (PIFA), nearly dou-

bling its electrical size. Therefore, adding a short strip can reduce the required size of the antenna for a given frequency (Liu *et al.*, 1997). The antenna is fed with a standard coaxial probe feed, and the locations of the feed point and the short strip would be expected to affect the tuning of the antenna. In this paper we will not discuss the effects of the feed locations and the short strip locations in detail. The location of the short strip is fixed at  $F=1.25 \text{ mm}$ , and the location of feed point at  $E=3.25 \text{ mm}$ .

Fig.3 shows the return loss characteristics ( $|S_{11}|$ ) as a function of frequency for the four positions of the GI tract. It was found that there was no obvious difference for input impedance bandwidths ( $|S_{11}| \leq -10 \text{ dB}$ ) between the four positions, which were all about 10 MHz (1.09%) for the proposed antenna. This indicates that the tissues and organs surrounding the proposed antenna have little effect on the bandwidths, and can result in the slight shift of the resonant frequency.

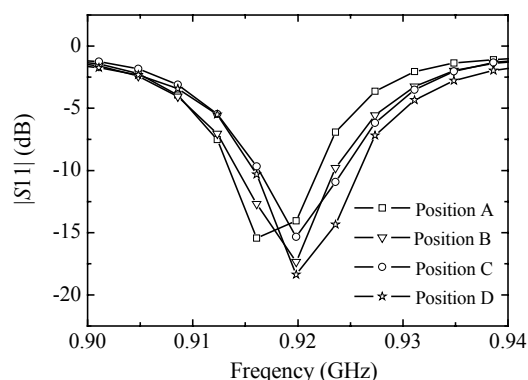
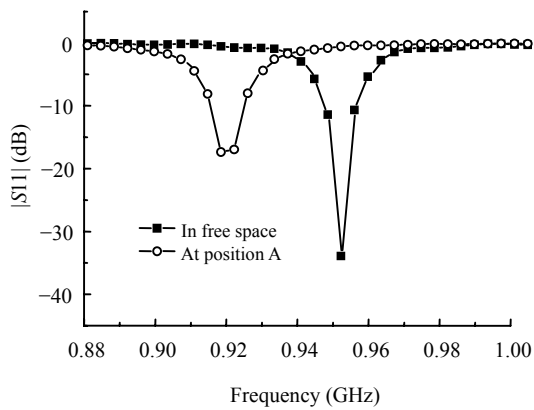


Fig.3 Comparison between return loss ( $|S_{11}|$ ) of the designed antenna as a function of the locations

However, in different positions, the tuning frequency was found to have a shift, and varied from 916 MHz to 920 MHz.

### Effect of human body on resonant frequency

When the encapsulated microstrip antenna is swallowed inside the GI tract, due to the dielectric loading effect, the antenna is de-tuned. The resonant frequency gets lowered and the return loss degrades due to an inductive effect in its impedance characteristics. Moreover, the dielectric loading effect is more pronounced at the higher frequency band. Fig.4 presents the resonant frequency characteristics of the ingested microstrip patch antenna in free space and at



**Fig.4 Comparison between return loss ( $|S_{11}|$ ) of the designed antenna in free space and inside the human body model**

position A of the human small intestine. It is shown that there is an offset of about 35 MHz between the resonant frequencies of the microstrip antenna operating in free space and that operating at position A of the human small intestine.

**Far-field pattern**

The  $x$ - $y$ -plane (horizontal) far-field patterns of the proposed antenna at the four positions are given in Fig.5. There were similarities in the patterns and magnitude of the horizontally polarized far fields ( $E_{\phi}$ ) at B and C. There existed four nulls in the patterns in the azimuth. For the ingested antenna at A and D, there were five nulls. Moreover the magnitudes of the horizontally polarized far fields at A and D are smaller than those at B and C.

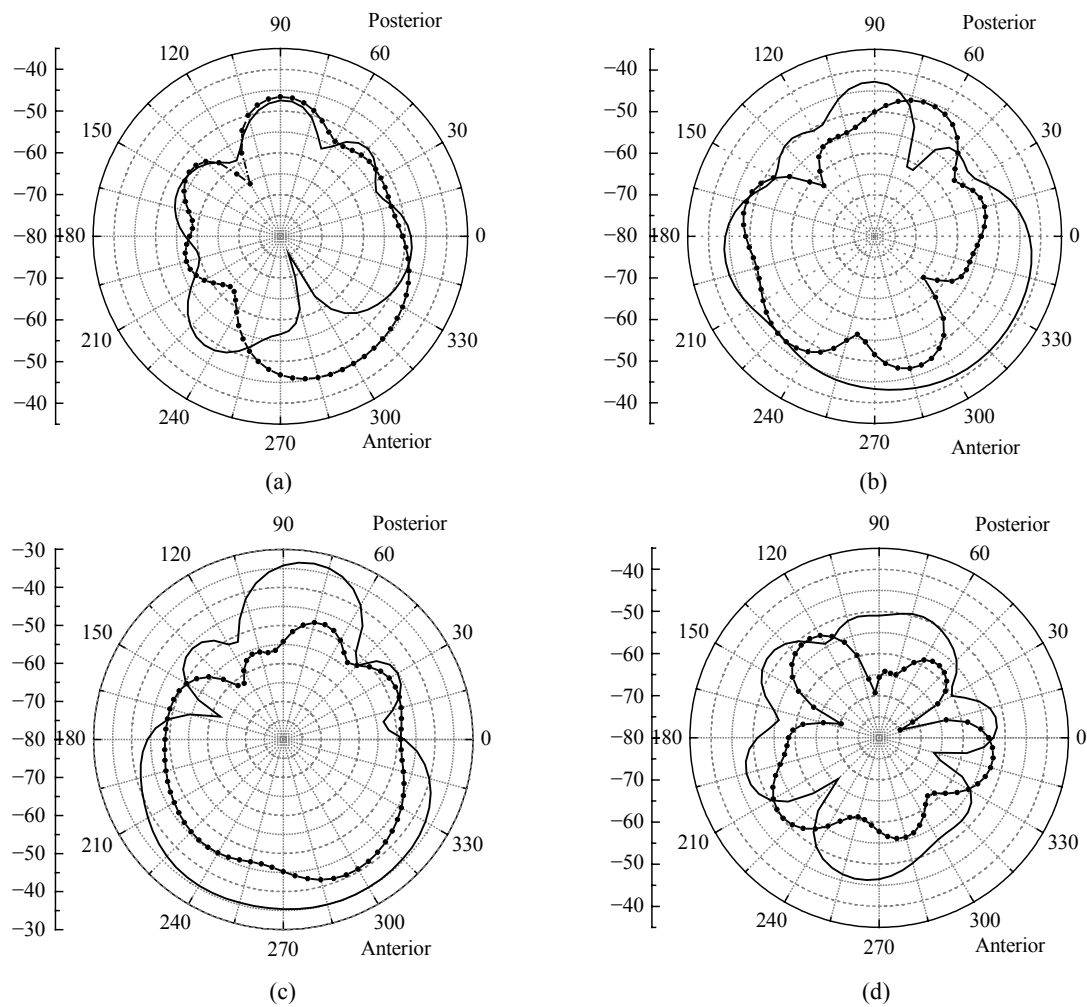


**Fig.5 Azimuthal far-field patterns of the proposed antenna at position A (a), position B (b), position C (c) and position D (d). Dotted line: vertically polarized pattern; solid line: horizontally polarized pattern**

The simulation results show that the maximum directivity is observed in the front of the human body, implying that the radiated field is predominantly strongest in the anterior direction (especially at the left of the abdomen centre). This indicates that if a single antenna was to be used as the receiving signal, it should be placed at this direction.

For the ingested antenna at A, the total field comprises mainly vertically polarized electric field ( $E_\theta$ ), while at B, C and D,  $E_\phi$  is greater than  $E_\theta$ .

### SAR COMPUTATIONS

SAR is the standard criteria to measure the amount of EM energy absorbed in the body. For harmonically varying EM fields, the SAR is defined as

$$SAR = \frac{\sigma}{2\rho} |\hat{E}|^2 = \frac{\sigma}{2\rho} (|\hat{E}_x|^2 + |\hat{E}_y|^2 + |\hat{E}_z|^2),$$

where  $\hat{E}_x$ ,  $\hat{E}_y$  and  $\hat{E}_z$  are the peak values of electric-field components,  $\rho$  is the mass density of the tissue in  $\text{kg/m}^3$  and  $\sigma$  is the conductivity in  $\text{s/m}$ . The

12-component approach is used for obtaining SAR in each cell. For calculating the peak spatial-average SAR, we chose a scheme presented in the IEEE guideline (IEEE Standard C95.1-1999, 1999).

When the antenna was normalized to a maximum transmitted power of 1 W, the 1-g SAR averaged distributions over the  $x$ - $y$  plane ( $z$ =the center of the antenna) for the proposed antenna at the four different positions are given in Fig.6. From Fig.6 we could find that the peak 1-g values of the four different positions are all recorded at the tissues surrounding the antenna and are 86.25 W/kg, 101.0 W/kg, 109.9 W/kg and 15.14 W/kg, respectively, which are much higher than the regulated SAR limitation of ANSI ( $SAR_{1-g} \leq 1.6 \text{ W/kg}$ ) (IEEE Standard C95.1-1999, 1999). This fact indicates that the delivered power of the proposed antenna embedded in the human body should be decreased to the proper levels, i.e. 14.5 mW (maximum available powers) for the compact microstrip antenna, with the SAR limitation being satisfied. Furthermore, the peak 1-g value of the position D is much smaller than those of other three positions, which are mainly attributed to the different dielectric properties of the esophagus compared with the small intestine.

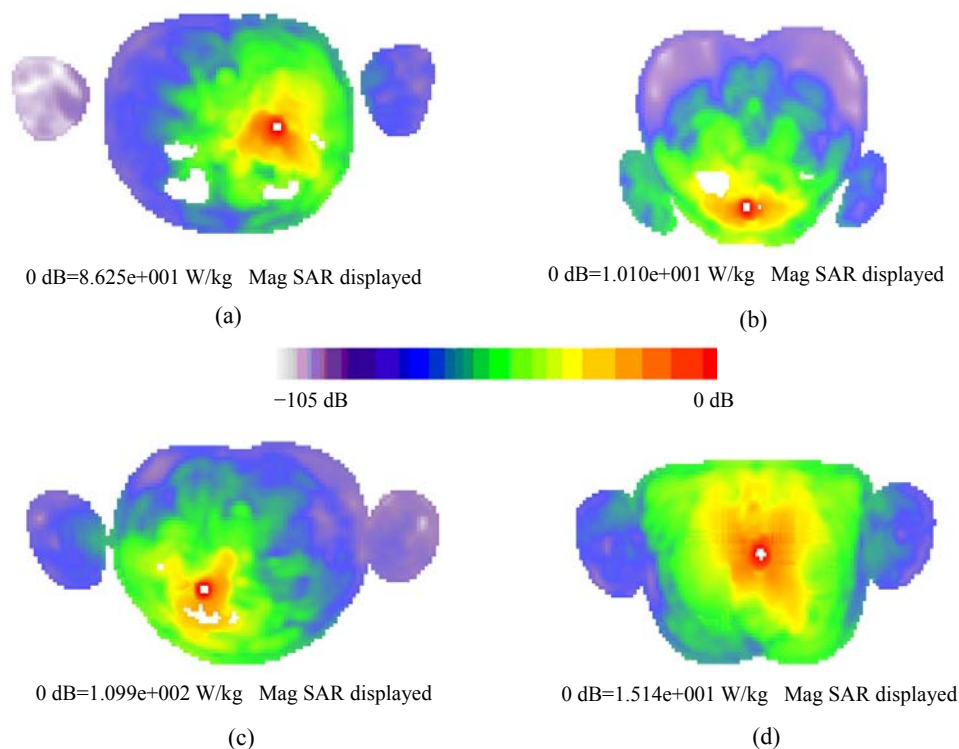


Fig.6 1-g SAR averaged distributions at position A (a), position B (b), position C (c) and position D (d)

In order to better identify the EM absorption characteristics in the major organs and four positions, the peak SAR values were calculated. We found that the peak SAR values averaged over 1-g and 10-g of the small intestine or the esophagus were much higher than those of other organs. This fact indicates that the majority of EM energy was absorbed by the small intestine or the esophagus surrounding the antenna. From Table 2, we could also find that the peak SAR values averaged over 1-g was greater than that over 10-g, implying that the absorption regions of the tissues and organs were intensive or condensed. This also implies a significant fact that the peak SAR values and the EM absorption are mainly related to the magnetic near field when an antenna is ingested in the alimentary canal. These are important considerations when designing the overall ingested antennas with attention given to SAR limitation.

## CONCLUSION

A novel four spiral slots microstrip antenna that can be used for implanted radiotelemetry capsule has been analyzed in free space and human GI tract at 915 MHz (ISM bands). Based on these analyses, several observations were made.

Firstly, the resonant frequency of the antenna varied from 916 MHz to 920 MHz at the four representative locations of the alimentary canal. Then we found that there is an offset of about 35 MHz between the resonant frequencies of the proposed antenna in free space and inside the human body. Moreover, the radiation patterns at different positions of the

alimentary canal are obviously different due to the different organs and tissues surrounding the antenna. It was also noted that the magnitude of electric fields in the anterior direction is greater than that in the posterior direction.

Finally, the maximum delivered power for the designed antenna was found so that the SAR values of the antenna satisfy ANSI limitations. The maximum available power, 14.5 mW calculated in Section 5 to satisfy the ANSI SAR limitation, can be used as the delivered power of the implanted transmitting antennas. Moreover, we found that the majority of the EM energy was absorbed by the tissues or organs surrounding the antenna.

When the transmitted power is fixed, the data rate is a function of the channel state and is usually varied in such a way as to keep the probability of bit error approximately constant. In the clinical applications of our radiocapsule, the transmitting power is fixed at 1 mW and the transmitted data rate is adaptive according to the channel state. Moreover, the adaptive data rate feature provides a significant improvement in system performance as compared to a system transmitting at a fixed data rate. However, there must have optimal transmitted power and optimal data rate over time-varying channels to keep a reliable communication link between the designed antenna and the exterior device. The analysis and results presented in this paper do not take this into account. Future work will be carried out to investigate this issue, enabling an optimal data rate to be found in terms of minimum power consumption for the entire radiotelemetry system.

**Table 2 Peak SAR values (unit: W/kg) averaged over 1-g (SAR) and 10-g (SAR) of the major organs and tissues in the abdomen**

Tissues	Peak SAR <sub>1-g</sub>				Peak SAR <sub>10-g</sub>			
	A	B	C	D	A	B	C	D
Skin	0.011	0.230	0.060	0.694	0.0014	0.033	0.020	0.071
Liver	0.415	0.119	6.245	0.296	0.1401	0.104	1.111	0.060
Fat	0.552	0.443	1.710	0.012	0.1349	0.194	0.339	0.061
Blood	0.152	0.006	0.060	1.560	0.0357	0.004	0.030	0.563
Muscle	0.080	0.500	0.831	0.156	0.0190	0.345	0.337	0.100
Stomach/esophagus	0.013	N/A	0.010	15.140	0.0053	N/A	0.002	3.950
Lung	0.001	N/A	N/A	0.379	0.0008	N/A	N/A	0.176
Kidney	0.070	N/A	0.005	N/A	0.0500	N/A	0.004	N/A
Small intestine	86.250	101.000	109.800	N/A	20.6770	19.950	12.310	N/A

## References

- Berenger, J.P., 1996. Perfectly matched layer for FDTD solution of wave structure interaction problems. *IEEE Trans. on Antennas and Propagation*, **44**:110-117. [doi:10.1109/8.477535]
- Chirwa, L.C., Hammond, P.A., Roy, S., Cumming, R.S., 2003. Electromagnetic radiation from ingested sources in the human intestine between 150 MHz and 1.2 GHz. *IEEE Trans. on Biomed. Eng.*, **50**(4):484-492. [doi:10.1109/TBME.2003.809474]
- Gabriel, C., Gabriel, S., Corthout, E., 1996. The dielectric properties of biological tissues: I. literature survey. *Phys. Med. Biol.*, **41**:2231-2249. [doi:10.1088/0031-9155/41/11/001]
- Gandhi, O.P., Lazzi, G., Furse, C.M., 1996. Electromagnetic absorption in the human head and neck for mobile telephones at 835 and 1900 MHz. *IEEE Trans. on Microwave Theory Techniques*, **44**:1884-1897. [doi:10.1109/22.539947]
- Gupta, K.C., 1988. *Microstrip Antenna Design*. Artech House, Norwood, p.41-65.
- Iddan, G., Meron, G., Glukhovsky, A., Swain, P., 2000. Wireless capsule endoscopy. *Nature*, **405**:417-418. [doi:10.1038/35013140]
- IEEE Standard C95.1-1999, 1999. Safety Levels with respect to Human Exposure to Radio Frequency Electromagnetic Fields 3 kHz to 300 GHz.
- Johannessen, E.A., Wang, L., Cathy, W., David, R.S.C., Jon, M.C., 2006. Biocompatibility of a lab-on-a-pill sensor in artificial gastrointestinal environments. *IEEE Trans. on Biomed. Eng.*, **53**(11):2333-2340. [doi:10.1109/TBME.2006.883698]
- Kim, J., Rahmat-Samii, Y., 2004. Implanted antennas inside a human body: simulations, designs, and characterizations. *IEEE Trans. on Microwave Theory Techniques*, **52**:1934-1943. [doi:10.1109/TMTT.2004.832018]
- Kim, J.M., Oh, D., Yoon, J., Cho, S., Kim, N., Cho, J., Kwon, Y., Cheon, C., Kim, Y.K., 2005. *In vitro* and *in vivo* measurement for biological applications using micro-machined probe. *IEEE Trans. on Microwave Theory Techniques*, **53**:3415-3421. [doi:10.1109/TMTT.2005.857116]
- Lazzi, G., Gandhi, O.P., Sullivan, D.M., 2000. Use of PML absorbing layers for the truncation of the head model in cellular telephone simulations. *IEEE Trans. on Microwave Theory Techniques*, **48**:2033-2039. [doi:10.1109/22.884192]
- Lin, J.C., 1975. Microwave properties of fresh mammalian brain tissues at body temperature. *IEEE Trans. on Biomed. Eng.*, **22**:74-79. [doi:10.1109/TBME.1975.324546]
- Liu, Z.D., Hall, P.S., Wake, D., 1997. Dual-frequency planar inverted-F antenna. *IEEE Trans. on Antennas and Propagation*, **45**:1451-1457. [doi:10.1109/8.633849]
- Pandolfino, J.E., Richter, J.E., Ours, T., Guardino, J.M., Chapman, J., Kahrilas, P.J., 2003. Ambulatory esophageal pH monitoring using a wireless system. *Am. J. Gastroenterol.*, **98**(4):740-749. [doi:10.1111/j.1572-0241.2003.07398.x]
- Scanlon, W.G., Evans, N.E., 2000. Radiowave propagation from a tissue implanted source at 418 MHz and 916.5 MHz. *IEEE Trans. on Biomed. Eng.*, **47**:527-534. [doi:10.1109/10.828152]
- Soontornpipit, P., Furse, C.M., You, C.C., 2004. Design of implantable microstrip antenna for communication with medical implants. *IEEE Trans. on Microwave Theory Techniques*, **52**:1944-1951. [doi:10.1109/TMTT.2004.831976]
- Wang, L., Johannessen, E.A., Hammond, P., Cui, L., Cooper, J.M., Reid, S.W.J., Cumming, D.R.S., 2005. A programmable microsystem using system-on-chip for real-time biotelemetry. *IEEE Trans. on Biomed. Eng.*, **52**(7):1251-1260. [doi:10.1109/TBME.2005.847562]
- Yee, K.S., 1966. Numerical solution of initial boundary value problems involving Maxwell's equations in isotropic media. *IEEE Trans. on Antennas and Propagation*, **14**(3):302-307. [doi:10.1109/TAP.1966.1138693]